Bioorganic & Medicinal Chemistry 22 (2014) 1029–1039

Contents lists available at ScienceDirect

Bioorganic & Medicinal Chemistry

journal homepage: www.elsevier.com/locate/bmc

Targeting the Warburg Effect in cancer; relationships for 2-arylpyridazinones as inhibitors of the key glycolytic enzyme 6-phosphofructo-2-kinase/2,6-bisphosphatase 3 (PFKFB3)

Darby G. Brooke [a], Ellen M. van Dam [b], Colin K. W. Watts [b], Amanda Khoury [b], Marie A. Dziadek [b], Hilary Brooks [b], Lisa-Jane K. Graham [b], Jack U. Flanagan [a,c], William A. Denny [a,c,*]

[a] Auckland Cancer Society Research Centre, School of Medical Sciences, The University of Auckland, Private Bag 92019, Auckland 1142, New Zealand
[b] Garvan Institute of Medical Research, 384 Victoria Street, Darlinghurst, Sydney, NSW 2010, Australia
[c] Maurice Wilkins Centre for Molecular Biodiscovery, The University of Auckland, Private Bag 92019, Auckland 1142, New Zealand

ARTICLE INFO

Article history:
Received 10 October 2013
Revised 5 December 2013
Accepted 17 December 2013
Available online 30 December 2013

Keywords:
Glycolysis
PFKFB3
Pyridazinone
Warburg Effect

ABSTRACT

High-throughput screening of a small-molecule library identified a 5-triazolo-2-arylpyridazinone as a novel inhibitor of the important glycolytic enzyme 6-phosphofructo-2-kinase/2,6-bisphosphatase 3 (PFKFB3). Such inhibitors are of interest due to PFKFB3's control of the important glycolytic pathway used by cancer cells to generate ATP. A series of analogues was synthesized to study structure-activity relationships key to enzyme inhibition. Changes to the triazolo or pyridazinone rings were not favoured, but limited-size substitutions on the aryl ring provided modest increases in potency against the enzyme. Selected analogues and literature-described inhibitors were evaluated for their ability to suppress the glycolytic pathway, as detected by a decrease in lactate production, but none of these compounds demonstrated such suppression at non-cytotoxic concentrations.

1. Introduction

It is well known that, even in the presence of oxygen, many cancer cells generate ATP from glucose primarily via glycolysis, rather than via the more efficient process of mitochondrial oxidative phosphorylation (respiration). This switch of energy metabolism in cancer cells to this process of 'aerobic glycolysis' (cf. normal cells favouring of glycolysis only under anaerobic conditions) is known as the Warburg Effect[1] and has been described as an 'emerging hallmark' of cancer.[2]

Despite the high rates of glycolysis maintained by malignant cells, which is exploited for ^{18}F-fluorodeoxyglucose-based PET imaging of tumours,[3] it nevertheless seems paradoxical that this significantly less efficient process (generating 2 ATP molecules per cycle) is preferred over oxidative phosphorylation (generating 36 ATP molecules per cycle). Current thinking, based on a 55 year-old hypothesis,[4] holds that this process enables the utilization of glycolytic metabolites as feedstock for other biosynthetic pathways, generating the organelles and macromolecules necessary for new cell formation, as well as antioxidants that are used to neutralize reactive oxygen species created during rapid cell proliferation.[5]

The rate-limiting enzyme in this process of conversion of glucose to pyruvate, the precursor of anaerobic ATP production, is considered to be 6-phosphofructo-1-kinase (PFK-1),[6] which converts fructose-6-phosphate (F6P) to fructose-1,6-bisphosphate (F1,6-BP). The activity of this enzyme is negatively regulated by ATP, but this regulation can be abrogated by the allosteric activator fructose-2,6-bisphosphate (F2,6-BP),[7,8] which is synthesised from F6P by the family of 6-phosphofructo-2-kinase/2,6-bisphosphatase (PFKFB) bifunctional enzymes. Of the four isoforms of this family, PFKFB3 is the most important in this context, with its kinase/phosphatase ratio of about 740:1 being the highest.[6,9] PFKFB3 (iPFK-2, PRG1) was originally identified as a progestin-regulated gene,[10] and is overexpressed in many cancer types including colon, prostate, pancreatic, breast, thyroid, and leukemia.[11] It is also induced by hypoxia, which is common in the tumour environment, through functional HIF (hypoxia-inducible factor) binding sites in the gene promoter.[12] PFKFB3 activity is also regulated by protein phosphorylation which occurs by a variety of signalling pathways relevant to cancer e.g., AMPK, PKA, PKC and PI3K/AKT.[13]

PFKFB3 has thus been of interest as a target for cancer therapy, and this has been validated by antisense and si/shRNA studies

Abbreviations: BCA, bicinchoninic acid assay; ECAR, extracellular acidification rate; PFKFB3, 6-phosphofructo-2-kinase/2,6-bisphosphatase 3; F6P, fructose-6-phosphate; PFK-1, 6-phosphofructo-1-kinase; F1,6-BP, fructose-1,6-bisphosphate; F2,6-BP, fructose-2,6-bisphosphate; RIPA, radioimmunoprecipitation assay; TEMPO, (2,2,6,2-tetramethylpiperidin-1-yl)oxy.

* Corresponding author. Tel.: +64 9 373 7599; fax: +64 9 373 7502.
E-mail address: b.denny@auckland.ac.nz (W.A. Denny).

0968-0896/$ - see front matter © 2013 Elsevier Ltd. All rights reserved.
http://dx.doi.org/10.1016/j.bmc.2013.12.041

which show decreased glycolysis in knock-down cell lines and tumor xenografts and inhibition of their proliferation[14–16] A number of compounds have been evaluated as potential inhibitors. Perhaps the most well-studied is 3-(3-pyridinyl)-1-(4-pyridinyl)-2-propen-1-one (3-PO; **1**), which has been reported as a modest inhibitor of isolated PFKFB3 enzyme (IC_{50} 25 ± 9 μM),[7] but also to suppress glycolytic flux, decrease the cellular concentrations of F2,6-BP and lactate, and to be cytostatic in both syngeneic and xenograft mouse models.[7] A more potent analogue (PFK-015) (**2**) has recently been reported and extensively evaluated,[17] although lactate secretion or other glycolytic endpoints were not determined. A series of benzo[*e*]indoles (e.g., **3**; PFK-095) has also been reported,[18] but only cell line inhibition data have been published on these.

A crystal structure of the human enzyme at 2.1 Å resolution showed the active pocket of the 6-phosphofructo-2-kinase domain existed in a rather rigid conformation, allowing independent binding of both F6P and ATP.[19] Computational screening of compounds using a 2.1 Å resolution crystal structure of PFKFB3 identified the chromenone (**4**) as a competitive inhibitor (IC_{50} 2.97 μM) of F6P, with a K_i of 1.29 μM.[20] A similarity search around **4** led to the 5-fold more potent chromene analogue **5** (IC_{50} 0.67 μM), which in HeLa cells resulted in a 40% decrease in F2,6-BP levels and a >30% decrease in lactate secretion on exposure at the IC_{50} for 8 h.[20] A combined pharmacophore screening/structure-based docking approach selected some compounds from the NCI Diversity Set II as likely actives,[21] and a recent patent[22] described a number of 4-sulfonamido-2-hydroxybenzoic acids, reported to inhibit PFKFKB3 with IC_{50}s from 0.2 to 11 μM; for example, **6** (KAN-222); IC_{50} (Kinase-Glo) 0.49 μM (Fig. 1).

In a search for drug-like inhibitors of PFKFB3, we conducted a high-throughput screen of 87,500 compounds (see Section 4.2.3 for details) and identified the triazolophenylpyridazinone **7** (Fig. 1), which showed low micromolar activity (IC_{50} 12 μM; Table 1) in a Kinase-Glo® assay for the enzyme. The synthesis of **7** has been published,[23] but no biology has been reported. In this Letter, we report the synthesis of range of analogues of **7**, and their structure-activity relationships as inhibitors of PFKFB3.

2. Results and discussion

2.1. Chemistry

The compounds of Tables 1–3 were prepared by the synthetic route outlined in Scheme 1. The starting materials 4,5-dibromopyridazin-3(2*H*)-one (**28**),[24] 4,5-diiodopyridazin-3(2*H*)-one (**29**)[25]

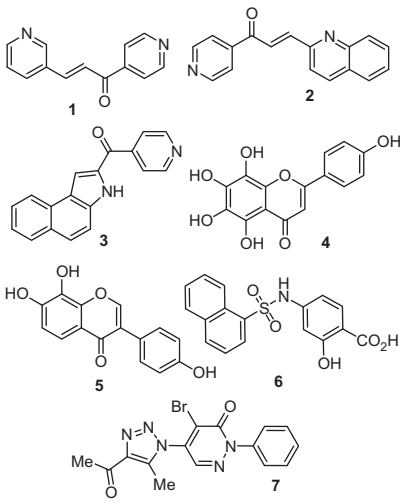

Figure 1. Structures of reported inhibitors of PFKFB3.

Table 1
Replacements for the acetyltriazole in compound **7**

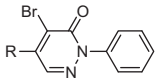

No	R	IC_{50}[a] (μM)
1	3-PO (Ref. 7)	26 ± 11
3	PFK095 (Ref. 14)	>1000[b]
6	KAN-222 (Ref. 18)	27 ± 19
7	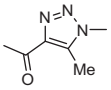	7.4 ± 4.8
8	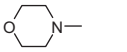	>1000
9	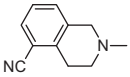	>500
10	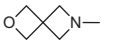	>1000
11	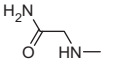	>1000
12	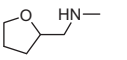	>1000

Footnotes for Table 1.
[a] Mean IC_{50} (μM) ± SD of at least 3 independent experiments (Kinase-Glo® assay).
[b] Compound **3** proved very insoluble, which may explain its inactivity in our hands.

and 2-phenyl-4,5-dibromopyridazin-3(2*H*)-one (**30**)[26] were known compounds, and 2-phenyl-4,5-dichloropyridazin-3(2*H*)-one (**31**) was commercially available. The other required analogues were accessed by one of three methods: (i) reaction of 4,5-dibromopyridazin-3(2*H*)-one (**28**) and substituted benzyl bromides **32**–**34**, using the conditions of Ryabtsova et al.[26] to give compounds **35**–**37** (Scheme 1A); (ii) reaction of the appropriate 4,5-dihalopyridazin-3(2*H*)-ones **28** and **29** with aryl boronic acids **38** and **39**, based on the method of Chang et al.[27] to give compounds **40**, **41** Scheme 1B); or (iii) reaction of appropriate arylhydrazines **42**–**44** with mucobromic acid (**45**) using the procedures of Devraj et al.[28] to give compounds **46**–**48**, Scheme 1C). Finally, 2-benzyl-5-bromopyridazin-3(2*H*)-one (**50**) was prepared[23] from 2-benzyl-4,5-dibromopyridazin-3(2*H*)-one (**49**), whilst Grignard treatment[26] of 2-phenyl-4,5-dibromopyridazin-3(2*H*)-one (**30**) gave 2-phenyl-4-isopropyl-5-bromopyridazin-3(2*H*)-one (**51**) (Scheme 1D).

The 2-substituted halopyridazin-3(2*H*)-ones were then converted to the corresponding azides with NaN_3 in DMF, using the conditions of Qian et al.[29] and these were sufficiently clean to be

Table 2
Replacements for the bromine in compound **7**

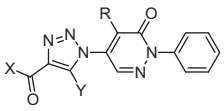

No	R	X,Y	IC_{50}[a] (μM)
13	Cl	Me, Me	26 ± 2
14	I	Me, Me	13 ± 3
15	$CHMe_2$	Me, Me	>500
16	OEt	Me, Me	>1000
17	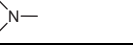	OEt, H	55 ± 16

Footnotes for Table 2.
[a] Mean IC_{50} (μM) ± SD of at least 3 independent experiments (Kinase-Glo® assay).

used without purification for the preparation of the compounds of Tables 1–3 (Scheme 2).

2.2. Structure–activity relationships

The ability of the compounds to inhibit human recombinant PFKFB3 was determined using a Kinase-Glo® assay (Promega), which measures enzyme activity by quantifying the amount of ATP remaining in solution following the kinase reaction. The presence of the GST tag had no effect on the kinase activity (data not shown). The known compound 3-PO (**1**) had an IC_{50} of 26 ± 1 μM in this assay, comparable with published data.[7] However, our IC_{50} value for **2** (>1000 μM) is not in agreement with the published[18] inhibitory data of 26% inhibition at 250 nM, possibly due to its very low solubility. Our IC_{50} value for **6** (27 μM) is also at variance with the published[19] value of 0.49 μM.

To explore the structure–activity relationships around compound **7**, we first examined the requirement for the acetyltriazole, which provides four polar atoms. Compounds **8**–**12** explored a number of alternatives for this moiety, including monocyclic (**8**), bicyclic (**9**, **10**) and acyclic (**11**, **12**) units with various polar substituents as replacement for the ketone, but all were inactive (Table 1).

Attention then turned to replacement of the bromine, which was seen as a potential metabolic liability (Table 2). Analogues with the smaller chloro (**13**) and larger iodo (**14**) halogens were about two-fold less active and equally active respectively (IC_{50}s 26 and 13 μM), suggesting the size of the substituent is relevant, which may indicate it contributes a halogen bond.[30] Interestingly, the isopropyl-(**15**) and ethoxy-(**16**) substituted analogues were much less active. Both of these substituents have similar bulk to an iodo group (the molar refractivities of I, OEt and iPr are 13.9, 12.5 and 17.1, respectively), but very different electronic properties (the Hammett sigma values for I, OEt and iPr being 0.18, −0.24 and −0.45, respectively),[31] suggesting that electron-donation to the pyridazone ring is not favoured. The moderately electron-donating spiromorpholine substituent in **17** did give better (albeit low) activity (IC_{50} 55 μM). However, this compound has a significantly different substitution pattern on the triazole ring (X = CO_2Et, not COMe and Y = H, not Me), so that direct comparison is difficult.

Table 3
Variations on the phenyl ring of compound **7**

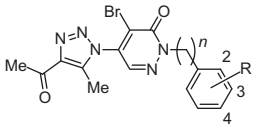

No	*n*	R	IC50[a] (μM)
18	0	4-CN	8.4 ± 8.1
19	0	4-OCF3	9.1 ± 3.2
20	0	4-Cl	7.0 ± 4.4
21	0	3,5-Diaza	9.6 ± 2.3
22	1	H	3.4 ± 4.7
23	1	H (des-Br)	>10,000
24	1	4-I	8.7 ± 2.4
25	2	H	2.6 ± 3.5
26	3	H	11 ± 6
27	1	4-NH(CH2)2NMe2	>500

Footnotes for Table 3.
[a] Mean IC_{50} (μM) ± SD of at least 3 independent experiments (Kinase-Glo® assay).

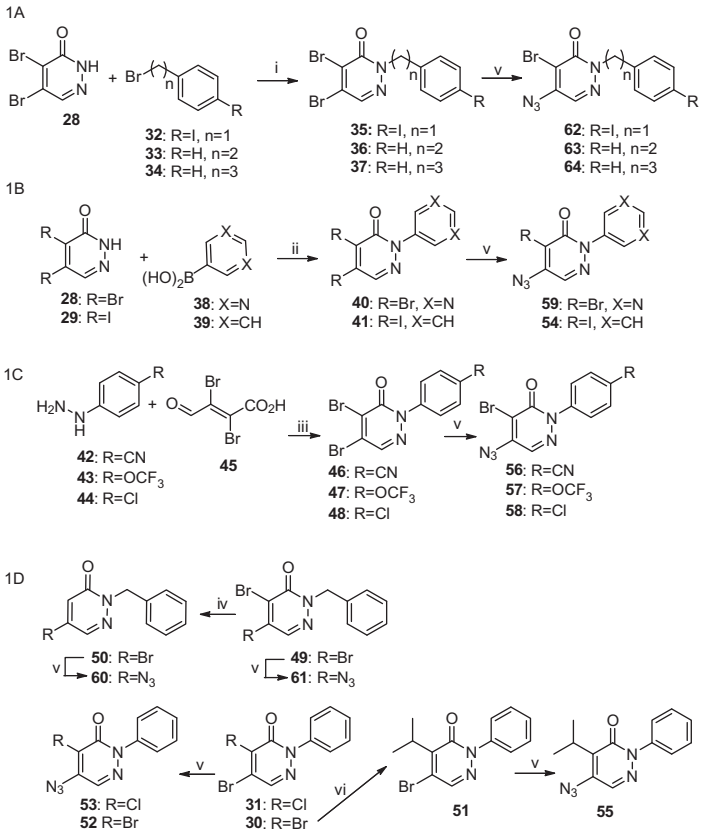

Scheme 1. Reagents and conditions: Syntheses of the azides required for preparation of the compounds of Tables 1–3. (i) K_2CO_3, $(n\text{-Bu})_4NBr$, MeCN, 16 h, 20 °C; (ii) TEMPO, $Cu(OAc)_2$, 4 Å molecular sieve, CH_2Cl_2, pyridine, 8.5 d, 20 °C; (iii) 6M HCl, 18 h, 65–95 °C; (iv); N_2H_4; (v) NaN_3, DMF, 2–3 h, 20 °C; (vi) (*i*-Pr)MgCl, THF, 3 min, −20 °C

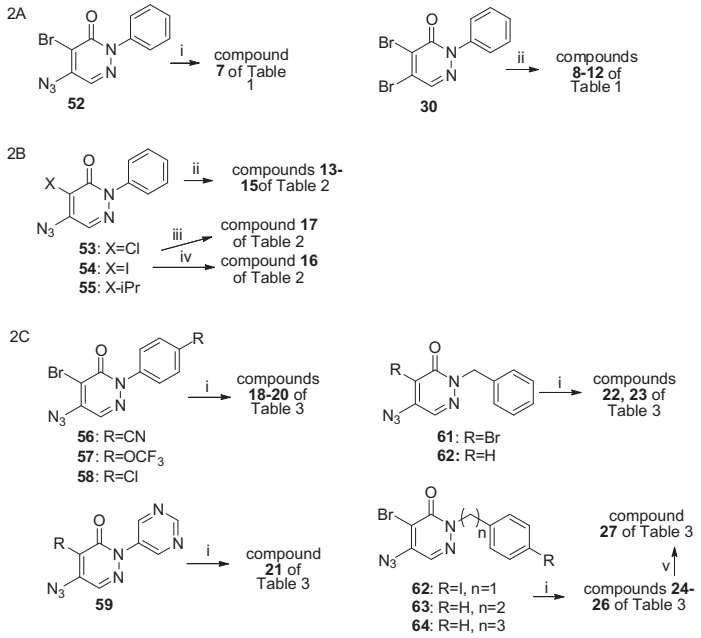

Scheme 2. Reagents and conditions: Syntheses of the compounds of Tables 1–3. (i) 2,4-pentanedione, NEt_3, dioxane, 1 h, 5–10 °C; (ii) RNH_2 or RRNH, EtOH, 1 h-10 days, 5-75 °C; (iii) ethyl propynoate, *N*,*N*-diisopropylethylamine, CuI, MeCN, 110 min, 20 °C, then 2-oxa-6-azaspiro[3.3]heptan-6-ium oxalate, *N*,*N*-diisopropylethylamine, 16 h, 20 °C; (iv) 2,4-pentanedione, K_2CO_3, EtOH, 1 h, 70–75 °C; (v) CuI, 2-dimethylaminoethylamine, L-proline, DMSO, 5 min, 95 °C. then K_2CO_3, 16 h, 95 °C.

The compounds in Table 3 explore variations on the phenyl ring. The results for compounds **18**–**20** and the diaza analogue **21** show that an electron-deficient phenyl ring (possessing electron-withdrawing groups or aza ring substitution) allows retention of potency. The activity of the benzyl analogue **22** (IC_{50} 3.4 μM) prompted the synthesis of the analogues **23**–**25**. The complete loss of activity with the des-bromo analogue **23** confirmed the results of Table 2 above, in that a sizeable substituent in this position is required for activity. The 4-iodo compound **24** retained activity, suggesting there is further bulk-tolerance in this region. Compound **27**, with a solubilising side chain at the 4-position, was thus prepared, but this was 100-fold less potent than **23**. To evaluate whether this loss of potency related to steric or polar attributes of this side chain, the phenethyl analogue **25** was prepared. This, with an IC_{50} of 2.6 μM, was the most potent compound prepared in the series, providing evidence of considerable bulk-tolerance for lipophilic substituents in this position. However, the propyl analogue **26** was 4-fold less potent than **25**, suggesting there are steric limits to this binding region.

To gain some insight into how **7** might interact with PFKFB3, a potential binding site and mode was predicted using molecular docking along with that for the recently crystallised **4**.[20] When challenged with a docking cavity that covered both the kinase ATP and F6P binding sites, the pose for **4** top ranked by the ChemPLP scoring function was located in the F6P site with the acetyltriazole phenyl moiety in close proximity to the side chain of Arg98 consistent with published data.[20] The top ranked mode predicted for **7** was also located in the F6P site (Fig. 2), with the terminal acetyltriazole group in a similar location to that predicted for the chromone-phenol of **4**, while its terminal phenyl group was placed in channel accessing bulk solvent defined by residues Thr48, Asn69, Arg75, Lys168, Ser171 and Tyr424.

The literature compounds **1** (3-PO) and **6** (KAN222), together with several of the more active PFKFB3 inhibitors in the 2-arylpyridazinone series (compounds **7**, **19**, **20**, **21** and **26**) were evaluated for their ability to inhibit glycolysis (and thus lactate production) in MDA-MB-231 cells at a concentration of 10 μM, using the Seahorse Bioscience XF24 cellular bioenergetics analyzer platform. In this system, inhibition of the glycolytic pathway is characterised by a decrease in the extracellular acidification rate (ECAR).[32] At 10 μM, neither **1** nor **7** showed any effect on ECAR (Fig. 3). In contrast, iodoacetate, which inhibits the glycolytic enzyme glyceraldehyde-3-phosphate dehydrogenase (GAPDH) decreased ECAR rapidly by ~75% (Fig. 3) and concomitantly increased the oxygen consumption rate (OCR, suggesting the stimulation of mitochondrial respiration) (data not shown). Some of the other 2-arylpyridazinones effected a small decrease in ECAR (~30% after 60 min), but there was also clear evidence of cytotoxicity (as shown by cell detachment) at this time. This could be due to an off-target effect, as iodoacetate and other glycolytic inhibitors showed no signs of cellular toxicity in the same time-frame.

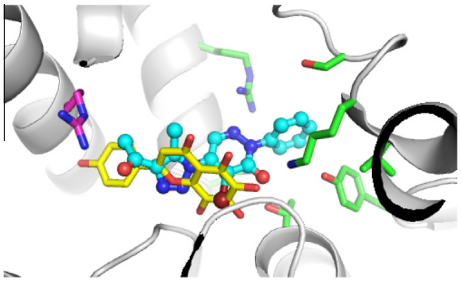

Figure 2. Predicted binding modes for **4** (yellow sticks) and **7** (cyan ball and stick) in the F6P binding site of the human PFKFB3 enzyme top ranked by the ChemPLP scoring function implemented in GOLD. Arg98 (magenta sticks) was reported to form a cation-π interaction with the phenol moiety of **4**.[20] Residues shown in green sticks indicate the channel in which the phenyl group of **7** was positioned.

3. Conclusions

The results show that the triazolophenylpyridazinone **7** is a modest inhibitor of PFKFB3, the key rate-controlling enzyme in the glycolytic pathway whereby cancer cells generate ATP. The structure–activity relationships for analogues of **7** show the presence of the triazolo and pyridazinone rings is key to their

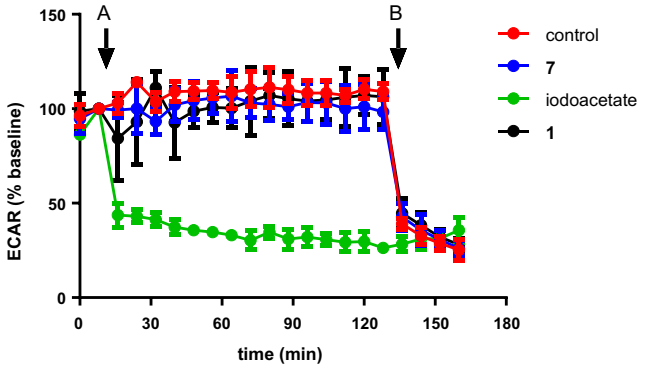

Figure 3. The impact of PFKFB3 and GAPDH inhibitors on glycolysis in MDA-MB-231 cells. After establishing a baseline ECAR, compounds **1**, **7** or iodoacetate were injected (arrow A) and ECAR was monitored for 120 min. 2-Deoxyglucose was then injected (arrow B) and ECAR was monitored for a further 32 min. Data is shown as means ± SD; $n = 3$ per treatment group.

inhibitory effect, and that modification on the pendant phenyl ring could significantly improve this activity. However, none of these analogues, or the known inhibitors **1** and **3**, showed evidence of being able to decrease lactate production in cells at non-cytotoxic concentrations. We are thus unable to conclude that the kinase-inhibitory activities of any of these compounds are related to inhibition of cellular PFKFB3, or whether the undoubted in vivo activity[7,17] of the literature compounds **1** and **6** is due to a different mechanism. However, only short-term effects of the compounds on glycolysis, i.e. within 6 h of administration of the compound, were measured. Depending on the half-life of F2,6BP, longer exposure to PFKFB3 inhibitors may be needed to measure an effect on the glycolytic pathways in MDA-MB-231 cells.

4. Experimental section

4.1. Chemistry

Unless otherwise stated, crude product mixtures were dissolved in a small volume of MeOH and/or EtOAc, and this mixture was then adsorbed on a small amount of silica gel, prior to purification by column chromatography on silica gel. Warming was often required to dissolve azide starting materials in dioxane. The regiochemistry of final products was confirmed by ^{1}H NMR observation of the nOe interaction between the pyridazinonyl H and triazolyl methyl (or analogous) groups. Experimental characterization data are provided for all new compounds, and for any literature compounds previously lacking full preparative and/or characterization data.

4.1.1. 4,5-Dibromo-2-(4-iodobenzyl)pyridazin-3(2*H*)-one (35) (Scheme 1A)

4,5-Dibromopyridazin-3(2*H*)-one (**28**) (7.753 g, 30.54 mmol, 1.00 equiv), 4-iodobenzyl bromide (**70**) (12.23 g, 41.19 mmol, 1.35 equiv), K_2CO_3 (11.150 g, 80.67 mmol, 2.64 equiv) and $(n\text{-Bu})_4NBr$ (310 mg, 0.96 mmol, 0.03 equiv) were stirred overnight at 20 °C in CH_3CN (100 mL), based on published conditions.[26] After ~24 h the reaction mixture was concentrated to dryness under reduced pressure, and the residue was re-suspended in CH_2Cl_2, filtered twice through a pad of Celite® and the filtrate was concentrated to dryness under reduced pressure. The product was re-precipitated from EtOAc/hexanes, to afford **35** (11.52 g, 80%) mp 144–146 °C; ^{1}H NMR ($CDCl_3$) δ 7.79 (s, 1H), 7.67 (m, 2H), 7.19 (m, 2H), 5.24 (s, 2H; HRESIMS calcd for $C_{11}H_8{}^{81}Br_2IN_2O$ m/z $[M+H]^+$ 472.8002, found 472.8004, calcd for $C_{11}H_8{}^{81}Br^{79}BrIN_2O$ m/z $[M+H]^+$ 470.8022, found 470.8025, calcd for $C_{11}H_8{}^{79}Br_2IN_2O$ for m/z $[M+H]^+$ 468.8043, found 468.8044; TLC $R_f = 0.49$ (20% EtOAc/hexanes).

4.1.2. 4,5-Dibromo-2-phenethylpyridazin-3(2*H*)-one (36)

Similar reaction of **28** (5.217 g, 20.55 mmol, 1.00 equiv) and (2-bromoethyl)benzene (**33**) (4.00 mL, 29.29 mmol, 1.43 equiv) for 24 h and workup gave a crude product that was re-precipitated from EtOAc to give **36** (1.529 g, 21%) as a microcrystalline white solid: mp 125-126 °C; ^{1}H NMR ($CDCl_3$): δ 7.76 (s, 1H), 7.29 (m, 2H), 7.23 (m, 3H), 4.39 (m, 2H), 3.10 (m, 2H); HRESIMS calcd for $C_{12}H_{10}{}^{81}Br_2N_2NaO$ m/z $[M+Na]^+$ 382.9012, found 382.9026, calcd for $C_{12}H_{10}{}^{81}Br^{79}BrN_2NaO$ m/z $[M+Na]^+$ 380.9032, found 380.9051, calcd for $C_{12}H_{10}{}^{79}Br_2N_2NaO$ for m/z $[M+Na]^+$ 378.9052, found 378.9066; TLC $R_f = 0.58$ (20% EtOAc/hexanes).

4.1.3. 4,5-Dibromo-2-(3-phenylpropyl)pyridazin-3(2*H*)-one (37)

Similar reaction of **28** (5.845 g, 23.02 mmol, 1.00 equiv) and 1-bromo-3-phenylpropane (**34**) (5.00 mL, 32.90 mmol, 1.43 equiv) for 43 h and workup gave a product that was purified by column chromatography on silica gel, eluting with 0–15% EtOAc/hexanes, to give **37** (6.177 g, 72%) as a pale yellow oil: ^{1}H NMR ($CDCl_3$): δ 7.77 (s, 1H), 7.28 (m, 2H), 7.18 (m, 3H), 4.21 (m, 2H), 2.70 (m, 2H), 2.16 (m, 2H); HRESIMS calcd for $C_{13}H_{12}{}^{81}Br_2N_2NaO$ m/z $[M+Na]^+$ 396.9168, found 396.9177, calcd for $C_{13}H_{12}{}^{81}Br^{79}BrN_2NaO$ m/z $[M+Na]^+$ 394.9189, found 394.9205, calcd for $C_{13}H_{12}{}^{79}Br_2N_2$-NaO for m/z $[M+Na]^+$ 392.9209, found 392.9221; TLC $R_f = 0.52$ (20% EtOAc/hexanes).

4.1.4. 4,5-Dibromo-2-(pyrimidin-5-yl)pyridazin-3(2*H*)-one (40) (Scheme 1B)

Following a published method,[27] **28** (10.123 g, 39.87 mmol, 1.00 equiv), pyrimidine-5-boronic acid (**37**) (24.90 g, 200.97 mmol, 5.40 equiv), TEMPO (18.50 g, 118.40 mmol, 2.97 equiv), $Cu(OAc)_2 \cdot H_2O$ (4.20 g, 21.04 mmol, 0.53 equiv) and powdered 4 Å molecular sieves (6.7 g) were combined in CH_2Cl_2 (300 mL). To this mixture was added pyridine (3.40 mL, 42.21 mmol, 1.06 equiv), and the resulting khaki suspension was stirred vigorously at 20 °C under N_2 for 15 min, and then under atmospheric air (via three needles in one of the septa capping the reaction vessel). A further quantity of pyridine (15.00 mL, 186.22 mmol, 4.67 equiv) was then added, causing an immediate change in the colour of the reaction mixture to a blue suspension, which became a green suspension after stirring overnight. The rate of stirring was decreased and the mixture was stirred at 20 °C for 8.5 days. The reaction was then filtered through a pad of Celite,® and the filtrate was diluted, washed with saturated aqueous NaOAc, and extracted with CH_2Cl_2 (×4). The combined organic extracts were washed (saturated aqueous $NaHCO_3$, dried, and concentrated to dryness under reduced pressure. The resulting viscous red semi-solid was triturated with 20% EtOAc/hexanes to give **40** (9.993 g) as a ~1:1 mixture with an unidentified impurity (probably starting material judged by ^{1}H NMR), and was used without further purification: ^{1}H NMR ($CDCl_3$): 10.77 (v br s, 1H), 9.23 (s, 1H), 9.16 (s, 2H), 8.03 (s, 1H), 7.84 (s, 1H); HRESIMS calcd for $C_8H_5{}^{81}Br_2N_4O$ m/z $[M+H]^+$ 334.8784, found 334.8801, calcd for $C_8H_5{}^{81}Br^{79}BrN_4O$ m/z $[M+H]^+$ 332.8804, found 332.8820, calcd for $C_8H_5{}^{79}Br_2N_4O$ m/z $[M+H]^+$ 330.8825, found 330.8832; TLC $R_f = 0.18$, 0.20 (20% EtOAc/hexanes).

4.1.5. 4,5-Diiodo-2-phenylpyridazin-3(2*H*)-one (41)

Similar reaction of 4,5-diiodopyridazin-3(2*H*)-one (**29**) (5.211 g, 14.98 mmol, 1.00 equiv) and phenylboronic acid (**38**) (3.67 g, 30.06 mmol, 2.01 equiv) in CH_2Cl_2 (150 mL) for 9 days, then filtered through a pad of Celite®. The filtrate was diluted and washed with saturated aqueous NH_4OAc, and the resulting mixture was then extracted with EtOAc (×4), and the combined organics were

washed, dried and evaporated to give an orange oil. This was re-precipitated from EtOAc/hexanes to afford **41** (1.752 g, 28%) as a yellow semi-crystalline solid: mp 122–124 °C; ^{1}H NMR ($CDCl_3$): 7.73 (s, 1H), 7.56 (m, 2H), 7.49 (m, 2H), 7.43 (m, 1H); HRESIMS calcd for $C_{10}H_7I_2N_2O$ *m*/*z* $[M+H]^+$ 424.8642, found 424.8653; TLC R_f = 0.52 (20% EtOAc/hexanes).

4.1.6. 4-(4,5-Dibromo-6-oxopyridazin-1(6*H*)-yl)benzonitrile (46) (Scheme 1C)

A suspension of 4-hydrazinylbenzonitrile hydrochloride (**42**) (9.360 g, 55.19 mmol, 1.25 equiv) in 6M HCl (220 mL) was added to a solution/suspension of mucobromic acid (**45**) (11.430 g, 44.32 mmol, 1.00 equiv) in 6M HCl (300 mL), and the resulting suspension was stirred at 65–95 °C for 18 h, when TLC analysis indicated the reaction was complete.[28] The viscous canary yellow suspension was cooled to 20 °C and the solid was collected by filtration and washed sequentially with water and hexanes. The dried crude product was triturated with MeOH to furnish **46** (10.047 g, 64%) as an amorphous off-white solid: mp 263–265 °C; ^{1}H NMR (DMSO-d_6): δ 8.34 (s, 1H), 8.02 (d, J = 8.53 Hz, 2H), 7.80 (d, J = 8.53 Hz, 2H); HRESIMS calcd for $C_{11}H_5{}^{81}Br_2N_3NaO$ *m*/*z* $[M+Na]^+$ 379.8651, found 379.8649, calcd for $C_{11}H_5{}^{81}Br^{79}BrN_3NaO$ *m*/*z* $[M+Na]^+$ 377.8671, found 377.8661, calcd for $C_{11}H_5{}^{79}Br_2N_3NaO$ for *m*/*z* $[M+Na]^+$ 375.8692, found 375.8694; TLC R_f = 0.38 (20% EtOAc/hexanes).

4.1.7. 4,5-Dibromo-2-(4-(trifluoromethoxy)phenyl)pyridazin-3(2*H*)-one (47)

Similar reaction of a suspension of (4-(trifluoromethoxy)phenyl)hydrazine hydrochloride (**43**) (15.330 g, 67.06 mmol, 1.21 equiv) in 6M HCl (100 mL) and **45** (14.300 g, 55.45 mmol, 1.00 equiv) in 6M HCl (360 mL) for 30 min. More 6M HCl (250 mL), H_2O (100 mL) and a portion of cHCl (50 mL) were then added and the reaction was continued for a further 16 h at 85–100 °C, when TLC showed the reaction was compete. The cooled mixture was filtered to give a dark orange solid that was washed with Et_2O and triturated with hexanes to give **47** (4.327 g) as an amorphous white solid: mp 138–140 °C. Further workup of the Et_2O layer gave more **47** (5.375 g) for an overall yield of 35%.; ^{1}H NMR ($CDCl_3$): δ 7.95 (s, 1H), 7.66 (m, 2H), 7.33 (m, 2H); HRESIMS calcd for $C_{11}H_5{}^{81}Br_2F_3N_2NaO_2$ *m*/*z* $[M+Na]^+$ 438.8522, found 438.8556, calcd for $C_{11}H_5{}^{81}Br^{79}BrF_3N_2NaO_2$ *m*/*z* $[M+Na]^+$ 436.8542, found 436.8568, calcd for $C_{11}H_5{}^{79}Br_2F_3N_2NaO_2$ *m*/*z* $[M+Na]^+$ 434.8562, found 434.8586; TLC R_f = 0.56 (20% EtOAc/hexanes).

4.1.8. 4,5-Dibromo-2-(4-chlorophenyl)pyridazin-3(2*H*)-one (48)

Similar reaction of (4-chlorophenyl)hydrazine hydrochloride (**44**) (9.80 g, 54.74 mmol, 1.20 equiv) in 6M HCl (250 mL) and **45** (11.763 g, 45.61 mmol, 1.00 equiv) in 6M HCl (300 mL) for 32 h and workup gave a solid that was collected by filtration and triturated with Et_2O to give **48** (11.797 g, 71%) as an apricot-tan solid: mp 181–182 °C; ^{1}H NMR ($CDCl_3$): δ 7.93 (s, 1H), 7.70 (m, 2H), 7.45 (m, 2H); HRESIMS calcd for $C_{10}H_5{}^{81}Br_2ClN_2NaO$ *m*/*z* $[M+Na]^+$ 388.8308, found 388.8274, calcd for $C_{10}H_5{}^{81}Br^{79}BrClN_2NaO$ *m*/*z* $[M+Na]^+$ 386.8328, found 386.8303, calcd for $C_{10}H_5{}^{79}Br_2ClN_2NaO$ *m*/*z* $[M+Na]^+$ 384.8349, found 384.8324; TLC R_f = 0.59 (20% EtOAc/hexanes).

4.1.9. 2-Phenyl-4-isopropyl-5-bromopyridazin-3(2*H*)-one (51) (Scheme 1D)

Using a published method,[26] a solution of 2-phenyl-4,5-dibromopyridazin-3(2*H*)-one (**30**) (1.043 g, 3.16 mmol, 1.00 equiv) in THF (23 mL) was cooled to −20 °C and treated with one portion of (*i*-Pr)MgCl (2M in THF, 1.58 mL, 3.16 mmol, 1.00 equiv) to give a very dark red–brown solution. After exactly 3 min the reaction was quenched by addition of water (0.570 μL, 31.61 mmol, 10.00 equiv), allowed to warm to 20 °C over 145 min, then poured into saturated aqueous NH_4Cl solution. The mixture was extracted with CH_2Cl_2 (×4), and the combined extracts were dried ($MgSO_4$) and concentrated to dryness under reduced pressure. The dark orange residue was purified by column chromatography on silica gel, eluting with 0–30% EtOAc/hexanes, to give **51** (0.229 g, 25%) as a yellow oil: ^{1}H NMR ($CDCl_3$): 7.91 (s, 1H), 7.54 (m, 2H), 7.47 (m, 2H), 7.39 (m, 1H), 3.48 (sept, J = 6.9 Hz, 1H), 1.40 (d, J = 7.0 Hz, 6H); LRMS (APCI+): *m*/*z* $[M+H]^+$ 295.4 (^{81}Br, 80%), 293.4 (^{79}Br, 100%); TLC R_f = 0.70 (20% EtOAc/hexanes).

4.1.10. General procedure for the preparation of azides (Scheme 1)

Based on a published method,[29] pyridazinones and NaN_3 were combined in dry DMF, and the resulting solution stirred at 20 °C under air (via two needles in the septum capping the reaction vessel). When analysis of an aliquot of the reaction by TLC (azides were generally more polar on TLC than their bromide precursors) and LRMS indicated the reaction was complete (typically after 2–3 h) the reaction mixture was concentrated to dryness under reduced pressure, and the resulting oily residue triturated with water to give an amorphous solid. This material was collected by filtration, washed with hexanes, and finally dried under high vacuum to give the azide as an amorphous solid. Azides were stored in the dark under N_2 at ~4 °C, and used as soon as possible. Due to safety concerns, melting-point measurements of these compounds were not obtained. In this way were prepared:

4.1.11. 5-Azido-4-bromo-2-phenylpyridazin-3(2*H*)-one (52)

As an amorphous tan solid, 91% yield; ^{1}H NMR ($CDCl_3$): δ 7.74 (s, 1H), 7.56 (m, 2H), 7.48 (m, 2H), 7.41 (m, 1H); LRMS (APCI+): *m*/*z* $[M+H]^+$ 294.3 (^{81}Br, 40%), 292.3 (^{79}Br, 40%); TLC R_f = 0.36 (20% EtOAc/hexanes).

4.1.12. 5-Azido-4-chloro-2-phenylpyridazin-3(2*H*)-one (53)

As an amorphous yellow–orange solid, 92% yield; ^{1}H NMR ($CDCl_3$): δ 7.75 (s, 1H), 7.57 (m, 2H), 7.48 (m, 2H), 7.42 (m, 1H); LRMS (APCI+): *m*/*z* $[M+H]^+$ 250.3 (^{81}Br, 35%), 248.3 (^{79}Br, 100%); TLC R_f = 0.38 (20% EtOAc/hexanes).

4.1.13. 5-Azido-4-iodo-2-phenylpyridazin-3(2*H*)-one (54)

As an amorphous beige–yellow solid, ~100% yield; ^{1}H NMR ($CDCl_3$): δ 7.66 (s, 1H), 7.56 (m, 2H), 7.47 (m, 2H), 7.41 (m, 1H); LRMS (APCI+): *m*/*z* $[M+H]^+$ 340.4 (65%); TLC R_f = 0.35 (20% EtOAc/hexanes).

4.1.14. 5-Azido-4-isopropyl-2-phenylpyridazin-3(2*H*)-one (55)

As a pale orange oil, 52% yield; ^{1}H NMR ($CDCl_3$): δ 7.83 (s, 1H), 7.55 (m, 2H), 7.46 (m, 2H), 7.38 (m, 1H), 3.39 (sept, J = 7.0 Hz, 1H), 1.32 (d, J = 7.0 Hz, 6H); LRMS (APCI+): *m*/*z* $[M+H]^+$ 256.5 (30%); TLC R_f = 0.50 (20% EtOAc/hexanes).

4.1.15. 4-(4-Azido-5-bromo-6-oxopyridazin-1(6*H*)-yl)benzonitrile (56)

As an amorphous dull yellow solid, ~100% yield; ^{1}H NMR ($CDCl_3$): δ 7.87 (m, 5H); LRMS (APCI+): *m*/*z* $[M+H]^+$ 319 (^{81}Br, 10%), 317 (^{79}Br, 10%), *m*/*z* $[(M-N_3+OH]^+$ 293.3 (^{81}Br, 90%), 291.3 (^{79}Br, 100%); TLC R_f = 0.11 (20% EtOAc/hexanes), 0.70 (50% EtOAc/hexanes)

4.1.16. 5-Azido-4-bromo-2-(4-(trifluoromethoxy)phenyl) pyridazin-3(2*H*)-one (57)

As an amorphous dull yellow solid, 71% yield; ^{1}H NMR ($CDCl_3$): δ 7.75 (s, 1H), 7.65 (m, 2H), 7.32 (m, 2H); LRMS (APCI+): *m*/*z*

$[M+H]^+$ 378.3 (^{81}Br, 80%), 376 (^{79}Br, 80%); TLC R_f = 0.35 (20% EtOAc:hexanes).

4.1.17. 5-Azido-4-bromo-2-(4-chlorophenyl)pyridazin-3(2*H*)-one (58)

As an amorphous yellow–tan solid, 94% yield; ^{1}H NMR ($CDCl_3$): δ 7.74 (s, 1H), 7.55 (m, 2H), 7.44 (m, 2H); LRMS (APCI+): *m*/*z* $[M+H]^+$ 328.3 (^{81}Br, 60%), 326 (^{79}Br, 40%); TLC R_f = 0.39 (20% EtOAc/hexanes).

4.1.18. 5-Azido-4-bromo-2-(pyrimidin-5-yl)pyridazin-3(2*H*)-one (59)

As an amorphous solid, 80% yield (estimated as ~70% pure by comparison of ^{1}H NMR integral ratios); ^{1}H NMR ($CDCl_3$): δ 9.22 (s, 1H), 9.15 (s, 2H), 7.82 (s, 1H); LRMS (APCI+): *m*/*z* $[M+H]^+$ 296 (^{81}Br, 55%), 294 (^{79}Br, 60%); TLC R_f = 0.03 (20% EtOAc/hexanes), 0.21 (40% EtOAc/hexanes).

4.1.19. 5-Azido-2-benzyl-4-bromopyridazin-3(2*H*)-one (60)

As an amorphous butter yellow solid, 76% yield; ^{1}H NMR ($CDCl_3$): δ 7.61 (s, 1H), 7.44 (m, 2H), 7.32 (m, 3H), 5.33 (s, 2H); LRMS (APCI+): *m*/*z* $[M+H]^+$ 308 (^{81}Br, 50%), 306.2 (^{79}Br, 55%); TLC R_f = 0.39 (20% EtOAc/hexanes).

4.1.20. 5-Azido-2-benzylpyridazin-3(2*H*)-one (61)

As a crystalline yellow solid, ~100% yield (estimated as ~65% pure by comparison of ^{1}H NMR integral ratios) and was used without further purification. TLC R_f = 0.24 (20% EtOAc/hexanes).

4.1.21. 5-Azido-4-bromo-2-(4-iodobenzyl)pyridazin-3(2*H*)-one (62)

As an amorphous beige–yellow solid, 76% yield; ^{1}H NMR ($CDCl_3$): δ 7.66 (m, 2H), 7.60 (s, 1H), 7.19 (m, 2H), 5.26 (s, 2H); LRMS (APCI+): *m*/*z* $[M+H]^+$ 434 (^{81}Br, 100%), 432.5 (^{79}Br, 100%); TLC R_f = 0.35 (20% EtOAc/hexanes).

4.1.22. 5-Azido-4-bromo-2-phenethylpyridazin-3(2*H*)-one (63)

As an off-white amorphous solid, ~100% yield; ^{1}H NMR ($CDCl_3$): δ 7.57 (s, 1H), 7.30 (m, 2H), 7.23 (m, 3H), 4.42 (m, 2H), 3.10 (app t, *J* = 7.8 Hz, 2H); LRMS (APCI+): *m*/*z* $[M+H]^+$ 322.4 (^{81}Br, 100%), 320 (^{79}Br, 100%); TLC R_f = 0.38 (20% EtOAc/hexanes).

4.1.23. 5-Azido-4-bromo-2-(3-phenylpropyl)pyridazin-3(2*H*)-one (64)

As a yellow crystalline solid, ~100% yield; ^{1}H NMR ($CDCl_3$): δ 7.58 (s, 1H), 7.28 (m, 2H), 7.18 (m, 3H), 4.23 (app t, *J* = 7.2 Hz, 2H), 2.69 (app t, *J* = 7.6 Hz, 2H), 2.15 (app pent., *J* = 7.4 Hz, 2H); LRMS (APCI+): *m*/*z* $[M+H]^+$ 336 (^{81}Br, 90%), 334.5 (^{79}Br, 100%); TLC R_f = 0.34 (20% EtOAc/hexanes).

4.1.24. 5-(4-Acetyl-5-methyl-1*H*-1,2,3-triazol-1-yl)-4-bromo-2-phenylpyridazin-3(2*H*)-one (7) (Table 1)

Using a literature general method,[23] 2,4-pentanedione (0.33 mL, 3.21 mmol, 0.99 equiv) and triethylamine (0.45 mL, 3.23 mmol, 1.00 equiv) were combined, and cooled to 0 °C (bath temperature). To the resulting solution was added, dropwise, a solution of azide **52** (944 mg, 3.23 mmol, 1.00 equiv) in dry dioxane (4.00 mL), and the resulting mixture was stirred at 0 °C for 9 min, after which it became too viscous. The reaction temperature was maintained between 5–10 °C for the 1 h, then warmed to 20 °C, diluted with Et_2O, and then filtered. The dried solid was purified by column chromatography on silica gel, eluting with 0–50% EtOAc/hexanes, followed by re-precipation from EtOAc/hexanes, to give **7** (366 mg, 30%) as a white microcrystalline solid: mp 208–210 °C (lit.[19]) 206–207 °C); ^{1}H NMR ($CDCl_3$): δ 7.89 (s, 1H), 7.66 (m, 2H), 7.52 (m, 3H), 2.79 (s, 3H), 2.66 (s, 3H); HRESIMS calcd for $C_{15}H_{12}{}^{81}BrN_5NaO_2$ *m*/*z* $[M+Na]^+$ 398.0047, found 398.0043; calcd for $C_{15}H_{12}{}^{79}BrN_5NaO_2$ *m*/*z* $[M+Na]^+$ 396.0067, found 396.0064; TLC R_f = 0.10 (20% EtOAc/hexanes), 0.67 (50% EtOAc/hexanes); HPLC purity: 99.9%.

4.1.25. 4-Bromo-5-morpholino-2-phenylpyridazin-3(2*H*)-one (8)

Following a general literature method,[33] 4,5-dibromo-2-phenylpyridazin-3(2*H*)-one (**30**) (1.067 g, 3.23 mmol, 1.00 equiv) and morpholine (0.590 mL, 6.75 mmol, 2.09 equiv) were heated under reflux in dry EtOH (33.0 mL) for 19 h. The reaction was cooled to 20 °C and partially concentrated under reduced pressure to give **8** (677 mg, 62%) as off-white crystals which was collected by filtration: mp 157–158 °C (lit.[27] 151–152 °C); ^{1}H NMR ($CDCl_3$): δ 7.66 (s, 1H), 7.57 (m, 2H), 7.46 (m, 2H), 7.38 (m, 1H), 3.89 (m, 4H), 3.47 (m, 4H); HRESIMS calcd for $C_{14}H_{14}{}^{81}BrN_3NaO_2$ *m*/*z* $[M+Na]^+$ 360.1047, found 360.1067, calcd for $C_{14}H_{14}{}^{79}BrN_3NaO_2$ *m*/*z* $[M+Na]^+$ 358.0162, found 358.0183; TLC R_f = 0.27 (40% EtOAc/hexanes); HPLC purity: 99.9%.

4.1.26. 2-(5-Bromo-6-oxo-1-phenyl-1,6-dihydropyridazin-4-yl)-1,2,3,4-tetrahydroisoquinoline-5-carbonitrile (9)

A similar reaction of **30** (1.048 g, 3.18 mmol, 1.00 equiv) and 1,2,3,4-tetrahydroisoquinoline-5-carbonitrile (0.58 g, 3.69 mmol, 1.16 equiv) under reflux in EtOH (34 mL)for 16 h. Filtration while hot and purification of the precipitate by re-precipitation from MeOH gave **9** (41 mg). Further concentration of the filtrate and purification gave additional material (180 mg total, 14%): mp 172–174 °C; ^{1}H NMR ($CDCl_3$): δ 8.08 (s, 1H), 7.75 (m, 1H), 7.55 (d, *J* = 7.3 Hz, 1H), 7.50 (m, 4H), 7.43 (m, 2H), 4.75 (s, 2H), 3.84 (t, *J* = 5.8 Hz, 2H), 3.17 (t, *J* = 5.7 Hz, 2H); HRESIMS calcd for $C_{20}H_{15}{}^{81}BrN_4NaO$ *m*/*z* $[M+Na]^+$ 431.0302, found 431.0263, calcd for $C_{20}H_{15}{}^{81}BrN_4NaO$ *m*/*z* $[M+Na]^+$ 429.0321, found 429.0279; TLC R_f = 0.29 (40% EtOAc/hexEtOAc/hexanes); HPLC purity: 98.0%.

4.1.27. 4-Bromo-2-phenyl-5-(2-oxa-6-azaspiro[3.3]heptan-6-yl)pyridazin-3(2*H*)-one (10)

Following a general literature method,[34] a solution of **30** (540 mg, 1.64 mmol, 1.00 equiv) in DMF (50 mL) was treated with anhydrous Cs_2CO_3 (824 mg, 2.51 mmol, 1.53 equiv) and 2-oxa-6-azaspiro[3.3]heptan-6-ium oxalate[35] (720 mg, 2.50 mmol, 1.53 equiv) and the mixture was stirred at 50 °C for 16 h, then at 100 °C for 4 h. The cooled reaction mixture was diluted with brine and extracted with EtOAc (×5). The combined organic extracts were washed with water (×3) and brine, dried ($MgSO_4$) and evaporated under reduced pressure. The residue was triturated with EtOAc/hexanes to give **10** (246 mg, 45% yield) as fine off-white crystals: mp 214–217 °C; ^{1}H NMR ($CDCl_3$): δ 7.54 (m, 2H), 7.43 (m, 2H), 7.34 (m, 1H), 7.23 (s, 1H), 4.85 (s, 4H), 4.62 (s, 4H); HRESIMS calcd for $C_{15}H_{14}{}^{81}BrN_3NaO_2$ *m*/*z* $[M+Na]^+$ 372.0412, found 372.0155; calcd for $C_{15}H_{14}{}^{79}BrN_3NaO_2$ *m*/*z* $[M+Na]^+$ 370.0162, found 370.0157. TLC R_f = 0.05 (50% EtOAc/hexanes); HPLC purity: 98.1%.

4.1.28. 2-((5-Bromo-6-oxo-1-phenyl-1,6-dihydropyridazin-4-yl)amino)acetamide (11)

Similar reaction of **30** (1.005 g, 3.05 mmol, 1.00 equiv), glycinamide hydrochloride (0.70 g, 6.31 mol, 2.07 equiv), and pyridine (0.51 mL, 6.31 mmol, 2.07 equiv) was heated under reflux in a mixture of EtOH (41 mL) and DMF (5 mL). After 48 h starting material remained, so more glycinamide hydrochloride (2.98 equiv) and NEt_3 (2.60 mL, 18.65 mmol, 6.12 equiv) were added and the mixture was heated under reflux for a further 16 h. The cooled mixture was filtered through a pad of Celite® and the filtrate was diluted with brine, extracted with CH_2Cl_2 (×3) and the combined extracts were washed with brine, dried ($MgSO_4$) and evaporated under reduced pressure. The residue was re-precipitated from MeOH:EtOAc

to give **11** (77 mg, 8%) as an amorphous off-white solid: mp 216-219 °C; ^{1}H NMR ($CDCl_3$): δ 7.75 (s, 1H), 7.56 (br s, 1H), 7.47 (m, 4H), 7.39 (m, 1H), 7.24 (br s, 1H), 6.71 (m, 1H), 4.05 (d, J = 6.20 Hz, 2H); HRESIMS calcd for $C_{12}H_{11}{}^{81}BrN_4NaO_2$ m/z $[M+Na]^+$ 346.9938, found 346.9947, calcd for $C_{12}H_{11}{}^{79}BrN_4NaO_2$ m/z $[M+Na]^+$ 344.9958, found 344.9963; TLC R_f = 0.22 (10% MeOH:EtOAc); HPLC purity: 98.7%.

4.1.29. 4-Bromo-2-phenyl-5-(((tetrahydrofuran-2-yl)methyl)amino)pyridazin-3(2*H*)-one (12)

Similar reaction of **30** (1.073 g, 3.25 mmol, 1.00 equiv) and tetrahydrofurfuryl amine (0.70 mL, 6.78 mmol, 2.09 equiv) were heated under reflux in EtOH (32 mL) for 16 h, then cooled and purified by column column chromatography on silica gel, eluting with 0–60% EtOAc/hexanes. Re-precipitation of the major product from EtOAc/hexanes gave **12** (785 mg, 67%) as an off-white crystalline solid: mp 133–134 °C; ^{1}H NMR ($CDCl_3$): δ 7.70 (s, 1H), 7.57 (m, 2H), 7.44 (m, 2H), 7.35 (m, 1H), 5.23 (m, 1H), 4.14 (m, 1H), 3.93 (m, 1H), 3.83 (m, 1H), 3.57 (ddd, J = 9.8, 6.2, 3.5 Hz, 1H), 3.37 (m, 1H), 2.08 (m, 1H), 1.98 (m, 2H), 1.67 (m, 1H); HRESIMS calcd for $C_{15}H_{16}{}^{81}BrN_3NaO_2$ m/z $[M+Na]^+$ 374.0298, found 374.0299, calcd for $C_{15}H_{16}{}^{79}BrN_3NaO_2$ m/z $[M+Na]^+$ 372.0318, found 372.0319; TLC R_f = 0.18 (50% EtOAc/hexanes); HPLC purity: 99.7%.

4.1.30. 5-(4-Acetyl-5-methyl-1*H*-1,2,3-triazol-1-yl)-4-chloro-2-phenylpyridazin-3(2*H*)-one (13) (Table 2)

Using a literature general method,[23] 2,4-pentanedione (0.72 mL, 7.01 mmol, 1.00 equiv), triethylamine (0.98 mL, 7.03 mmol, 1.00 equiv) and azide **53** (1.746 g, 7.05 mmol, 1.00 equiv) in dry dioxane (8.8 mL) were reacted at between 5-10 °C for 60 min, then warmed to 20 °C, filtered and washed with Et_2O. Purification by column column chromatography on silica gel, eluting with 0–30% EtOAc/hexanes, gave **13** as a an amorphous white solid (0.612 g, 26%): mp 213–216 °C; ^{1}H NMR ($CDCl_3$): δ 8.01 (s, 1H), 7.66 (m, 2H), 7.55 (m, 2H), 7.49 (m, 1H), 2.78 (s, 3H), 2.65 (s, 3H); HRESIMS calcd for $C_{15}H_{12}{}^{37}ClN_5NaO_2$ m/z $[M+Na]^+$ 354.0543, found 354.0555; calcd for $C_{15}H_{12}{}^{35}ClN_5NaO_2$ m/z $[M+Na]^+$ 352.0572, found 352.0581; TLC R_f = 0.28 (30% EtOAc/hexanes); HPLC purity: 99.7%.

4.1.31. 5-(4-Acetyl-5-methyl-1*H*-1,2,3-triazol-1-yl)-4-iodo-2-phenylpyridazin-3(2*H*)-one (14)

2,4-Pentanedione (0.33 mL, 3.21 mmol, 1.01 equiv), triethylamine (0.44 mL, 3.16 mmol, 0.99 equiv) and azide **54** (1.077 g, 3.18 mmol, 1.00 equiv) were similarly reacted in dry dioxane (35.0 mL) at 5–10 °C for 155 min, then filtered through a pad of Celite® and the filtrate concentrated to dryness under reduced pressure. The residue was dried and then triturated with cold MeOH to afford a solid that was collected by filtration and washed with hexanes to give **14** (0.517 g, 40%) as a semi-crystalline cream solid: mp 218–220 °C; ^{1}H NMR ($CDCl_3$): δ 7.70 (s, 1H), 7.65 (m, 2H), 7.54 (m, 2H), 7.49 (m, 1H), 2.79 (s, 3H), 2.67 (s, 3H); HRESIMS calcd for $C_{15}H_{12}IN_5NaO_2$ m/z $[M+Na]^+$ 443.9928, found 443.9931; calcd for $C_{15}H_{13}IN_5O_2$ m/z $[M+H]^+$ 422.0108, found 422.0129; TLC R_f = 0.10 (20% EtOAc/hexanes); HPLC purity: 97.1%.

4.1.32. 5-(4-Acetyl-5-methyl-1*H*-1,2,3-triazol-1-yl)-4-isopropyl-2-phenylpyridazin-3(2*H*)-one (15)

2,4-Pentanedione (0.46 mL, 4,5 mmol, 11 equiv), triethylamine (0.20 mL, 1.40 mmol, 2.5 equiv) and azide **55** (103 mg, 0.40 mmol, 1.00 equiv) in dry dioxane (20.0 mL) were similarly reacted at 75 °C for 10 days, then evaporated to dryness under reduced pressure. The residue was purified by column chromatography on silica gel, eluting with 0–40% EtOAc/hexanes. The resulting product was further purified by trituration with cold MeOH and filtration of the resulting suspension through a pad of Celite®, followed by concentration of the filtrate to dryness under reduced pressure, yielding **15** (86 mg, 63%) as an amorphous brittle solid: mp 76–79 °C; ^{1}H NMR ($CDCl_3$): δ 7.69 (s, 1H), 7.63 (m, 2H), 7.52 (m, 2H), 7.45 (m, 1H), 2.78 (s, 3H), 2.64 (sep, J = 6.9 Hz, 1H), 2.61 (s, 3H), 1.30 (d, J = 6.9 Hz, 6H); HRESIMS calcd for $C_{18}H_{19}N_5NaO_2$ m/z $[M+Na]^+$ 360.1431, found 360.1428; calcd for $C_{18}H_{20}N_5O_2$ m/z $[M+Na]^+$ 338.1612, found 338.1623; TLC R_f = 0.61 (40% EtOAc/hexanes); HPLC purity: 96.6%.

4.1.33. 5-(4-Acetyl-5-methyl-1*H*-1,2,3-triazol-1-yl)-4-ethoxy-2-phenylpyridazin-3(2*H*)-one (16)

Based on a literature general method,[36] 2,4-pentanedione (0.21 mL, 2.06 mmol, 1.00 equiv), azide **53** (511 mg, 2.06 mmol, 1.00 equiv), and K_2CO_3 (903 mg, 6.53 mmol, 3.17 equiv) were combined in dry EtOH (7.7 mL) and heated at 70–75 °C for 60 min, then concentrated to dryness under reduced pressure. The residue was neutralized with 10% aqueous HCl solution, and the resulting mixture was extracted with EtOAc (×4). The combined organic extracts were dried ($MgSO_4$), and evaporated under reduced pressure. The residue was purified by column chromatography on silica gel, eluting with 0–60% EtOAc/hexanes, followed by re-precipitation of product from EtOAc/hexanes, to give **16** (8 mg, 1%) as an amorphous white solid: mp 100–102 °C; ^{1}H NMR ($CDCl_3$): δ 7.97 (s, 1H), 7.61 (m, 2H), 7.53 (m, 2H), 7.46 (m, 1H), 4.72 (q, J = 7.1 Hz, 2H), 2.77 (s, 3H), 2.59 (s, 3H), 1.27 (t, J = 7.0 Hz, 3H); HRESIMS calcd for $C_{17}H_{17}N_5NaO_3$ m/z $[M+Na]^+$ 362.1224, found 362.1221; TLC R_f = 0.67 (50% EtOAc/hexanes); HPLC purity: 99.6%.

4.1.34. Ethyl 1-(6-oxo-1-phenyl-5-(2-oxa-6-azaspiro[3.3]heptan-6-yl)-1,6-dihydropyridazin-4-yl)-1*H*-1,2,3-triazole-4-carboxylate (17)

Based on a general literature method,[37] ethyl propynoate (0.20 mL, 1.98 mmol, 1.20 equiv), *N*,*N*-diisopropylethylamine (0.60 mL, 3.44 mmol, 2.01 equiv) and CuI (16 mg, 0.085 mmol, 0.05 equiv) were added to a solution of azide **53** (0.407 g, 1.64 mmol, 1.00 equiv) in CH_3CN (4.00 mL), and the resulting dark orange–brown solution was stirred at 20 °C for 110 min, then concentrated to dryness under reduced pressure. The residue was washed with hot MeOH, and the insoluble yellow solid collected by filtration. MS analysis confirmed this material contained the desired triazole product, whilst ^{1}H NMR analysis showed it comprised a ~3:1 mixture of isomers, favouring the desired product.

A solution of crude triazole (182 mg, 0.53 mmol, 1.00 equiv) in DMF (17.00 mL) was treated successively with *N*,*N*-diisopropylethylamine (0.40 mL, 2.30 mmol, 4.37 equiv) and 2-oxa-6-azaspiro[3.3]heptan-6-ium oxalate[34] (311 mg, 1.08 mmol, 2.05 equiv) and the resulting mixture was stirred at 20 °C for 16 h, then concentrated to dryness under reduced pressure. The residue was re-suspended in MeOH, filtered through a pad of Celite®, and the filtrate was purified by column column chromatography on silica gel, eluting with 0–50% EtOAc/hexanes followed by re-precipitation (twice) from EtOAc/hexanes, to give **17** (51 mg, 24%) as an amorphous white solid: mp 238–240 °C; ^{1}H NMR ($CDCl_3$): δ 8.30 (s, 1H), 7.50 (m, 5H), 7.41 (m, 1H), 4.67 (br s, 4H), 4.51 (q, J = 7.15 Hz, 2H), 4.31 (br s, 4H), 1.47 (t, J = 7.14 Hz, 3H); HRESIMS calcd for $C_{20}H_{20}N_6NaO_4$ m/z $[M+Na]^+$ 431.1438, found 431.1433, calcd for $C_{20}H_{21}N_6O_4$ m/z $[M+H]^+$ 409.1619, found 409.1622; TLC R_f = 0.13 (50% EtOAc/hexanes); HPLC purity: 97.1%.

4.1.35. 4-(4-(4-Acetyl-5-methyl-1*H*-1,2,3-triazol-1-yl)-5-bromo-6-oxopyridazin-1(6*H*)-yl)benzonitrile (18) (Table 3)

Similar reaction of 2,4-pentanedione (0.26 mL, 2.53 mmol, 0.99 equiv), triethylamine (0.36 mL, 2.58 mmol, 1.01 equiv) and azide **56** (811 mg, 2.56 mmol, 1.00 equiv) in dry dioxane (45.2 mL) for 50 min, followed by filtration through Celite®, evaporation of the filtrate and purification of the residue by column chromatography on silica gel, eluting with 0–50% EtOAc/hexanes, followed by

re-precipitation from EtOAc/hexanes, gave **18** (126 mg total, 12%) as an amorphous yellow solid: mp 222–224 °C; ^{1}H NMR ($CDCl_3$): δ 7.94 (s, 1H), 7.90 (m, 2H), 7.84 (m, 2H), 2.79 (s, 3H), 2.67 (s, 3H); HRESIMS calcd for $C_{16}H_{11}{}^{81}BrN_6NaO_2$ *m/z* $[M+Na]^+$ 422.9999, found 422.9992, calcd for $C_{16}H_{11}{}^{79}BrN_6NaO_2$ *m/z* $[M+Na]^+$ 421.0019 found 421.0007; TLC R_f = 0.40 (40% EtOAc/hexanes); HPLC purity: 98.7%.

4.1.36. 5-(4-Acetyl-5-methyl-1*H*-1,2,3-triazol-1-yl)-4-bromo-2-(4-(trifluoromethoxy)phenyl)-pyridazin-3(2*H*)-one (19)

Similar reaction of 2,4-pentanedione (0.38 mL, 3.70 mmol, 1.02 equiv), triethylamine (0.51 mL, 3.66 mmol, 1.00 equiv) and azide **57** (1.370 g, 3.64 mmol, 1.00 equiv) in dry dioxane (22.0 mL) for 90 min, followed by filtration through Celite®, evaporation of the filtrate and trituration of the residue with cold MeOH gave **19** (0.338 g, 20%) as semi-crystalline yellow solid: mp 158-160 °C; ^{1}H NMR ($CDCl_3$): δ 7.91 (s, 1H), 7.75 (m, 2H), 7.38 (m, 2H), 2.79 (s, 3H), 2.66 (s, 3H); HRESIMS calcd for $C_{16}H_{11}{}^{81}BrF_3N_5NaO_3$ *m/z* $[M+Na]^+$ 481.9870, found 481.9857, calcd for $C_{16}H_{11}{}^{79}BrF_3N_5NaO_3$ *m/z* $[M+Na]^+$ 479.9890, found 479.9875; TLC R_f = 0.20 (20% EtOAc/hexanes); HPLC purity: 100%.

4.1.37. 5-(4-Acetyl-5-methyl-1*H*-1,2,3-triazol-1-yl)-4-bromo-2-(4-chlorophenyl)pyridazin-3(2*H*)-one (20)

2,4-Pentanedione (0.32 mL, 3.12 mmol, 0.97 equiv), triethylamine (0.44 mL, 3.16 mmol, 1.01 equiv) and azide **58** (1.022 g, 3.13 mmol, 1.00 equiv) in dry dioxane (22.0 mL) were reacted at 5–10 °C for 60 min, then warmed to 20 °C and filtered through a pad of Celite®. The filtrate was evaporated under reduced pressure and the residue was purified by column chromatography on silica gel, eluting with 0–40% EtOAc/hexanes, followed by re-precipitation from EtOAc/hexanes, to give **20** (0.056 g, 4%) as an amorphous white solid: mp 188–190 °C; ^{1}H NMR ($CDCl_3$): δ 7.89 (s, 1H), 7.65 (m, 2H), 7.51 (m, 2H), 2.78 (s, 3H), 2.66 (s, 3H); HRESIMS calcd for $C_{15}H_{11}N_5O_2{}^{37}Cl^{81}BrNa$ *m/z* $[M+Na]^+$ 433.9628, found 433.9622, calcd for $C_{15}H_{11}N_5O_2{}^{37}Cl^{79}BrNa$ and $C_{15}H_{11}N_5O_2{}^{35}Cl^{81}BrNa$ *m/z* $[M+Na]^+$ 431.9656, found 431.9642, calcd for $C_{15}H_{11}N_5O_2{}^{35}Cl^{79}BrNa$ *m/z* $[M+Na]^+$ 429.9677, found 429.9664; TLC R_f = 0.42 (30% EtOAc/hexanes); HPLC purity: 99.5%.

4.1.38. 5-(4-Acetyl-5-methyl-1*H*-1,2,3-triazol-1-yl)-4-bromo-2-(pyrimidin-5-yl)pyridazin-3(2*H*)-one (21)

Similar reaction of 2,4-pentanedione (1.32 mL, 12.86 mmol, 1.00 equiv), triethylamine (1.80 mL, 12.91 mmol, 1.00 equiv) and azide **59** (3.793 g, 12.90 mmol, 1.00 equiv) in dry dioxane (23 mL) for 105 min gave a heterogeneous mixture that was filtered. The filtrate was diluted with hexanes, concentrated to half its original volume, then filtered through Celite®. The filtrate was evaporated and purified by column chromatography on silica gel, eluting with 0-50% EtOAc/hexanes, followed by re-precipitation from EtOAc/hexanes, to give **21** (0.870 g, 12%) as an amorphous yellow solid: mp 174–177 °C; ^{1}H NMR ($CDCl_3$): δ 9.29 (s, 1H), 9.24 (s, 2H), 7.99 (s, 1H), 2.79 (s, 3H), 2.67 (s, 3H); HRESIMS calcd for $C_{13}H_{10}{}^{81}BrN_7NaO_2$ *m/z* $[M+Na]^+$ 399.9952, found 399.9941, $C_{13}H_{10}{}^{79}BrN_7NaO_2$ *m/z* $[M+Na]^+$ 397.9972, found 397.9958; TLC R_f = 0.20 (50% EtOAc/hexanes); HPLC purity: 98.2%.

4.1.39. 5-(4-Acetyl-5-methyl-1*H*-1,2,3-triazol-1-yl)-2-benzyl-4-bromopyridazin-3(2*H*)-one (22)

Similar reaction of 2,4-pentanedione (0.34 mL, 3.31 mmol, 1.02 equiv), triethylamine (0.45 mL, 3.23 mmol, 0.99 equiv) and azide **61** (0.998 g, 3.26 mmol, 1.00 equiv) in dry dioxane (17.0 mL) for 105 min was followed by filtration of the mixture. The filtrate was evaporated under reduced pressure and triturated with cold MeOH to give **22** (0.417 g, 33%) as an amorphous white solid: mp 154–156 °C, 152–154 °C; ^{1}H NMR ($CDCl_3$): δ 7.75 (s, 1H), 7.52 (m, 2H), 7.38 (m, 3H), 5.45 (s, 2H), 2.76 (s, 3H), 2.56 (s, 3H); HRESIMS calcd for $C_{16}H_{14}{}^{81}BrN_5NaO_2$ *m/z* $[M+Na]^+$ 412.0203, found 412.0201; calcd for $C_{16}H_{14}{}^{79}BrN_5NaO_2$ *m/z* $[M+Na]^+$ 410.0223, found 410.0217; TLC R_f = 0.53 (40% EtOAc/hexanes); HPLC purity: 97.9%.

4.1.40. 5-(4-Acetyl-5-methyl-1*H*-1,2,3-triazol-1-yl)-2-benzylpyridazin-3(2*H*)-one (23)

Similar reaction of 2,4-pentanedione (0.16 mL, 1.56 mmol, 1.01 equiv), triethylamine (0.21 mL, 1.50 mmol, 0.98 equiv) and azide **60** (0.348 g, 1.53 mmol, 1.00 equiv) in dry dioxane (4.0 mL) for 170 min, followed by evaporation of the mixture and trituration of the residue with cold MeOH gave **23** (0.131 g, 28%) as an amorphous white solid: mp 147–148 °C; ^{1}H NMR ($CDCl_3$): δ 8.24 (d, *J* = 2.6 Hz, 1H), 7.48 (m, 2H), 7.35 (m, 3H), 6.99 (d, *J* = 2.6 Hz, 1H), 5.39 (s, 2H), 2.74 (app d, *J* = 2.6 Hz, 6H); HRESIMS calcd for $C_{16}H_{15}N_5NaO_2$ *m/z* $[M+Na]^+$ 332.1118, found 332.1117; calcd for $C_{16}H_{16}N_5O_2$ *m/z* $[M+H]^+$ 310.1299, found 310.1296; TLC R_f = 0.04 (20% EtOAc/hexanes); HPLC purity: 99.8%.

4.1.41. 5-(4-Acetyl-5-methyl-1*H*-1,2,3-triazol-1-yl)-4-bromo-2-(4-iodobenzyl)pyridazin-3(2*H*)-one (24)

Similar reaction of 2,4-pentanedione (0.30 mL, 2.92 mmol, 0.99 equiv), triethylamine (0.41 mL, 2.94 mmol, 0.99 equiv) and azide **62** (1.281 g, 2.97 mmol, 1.00 equiv) in dry dioxane (43 mL) for 125 min, followed by filtration through Celite®, evaporation of the filtrate and purification of the residue by column chromatography on silica gel, eluting with 0–20% EtOAc/hexanes, followed by re-precipitation from EtOAc/hexanes, gave **24** (0.677 mg, 44%) as an amorphous white solid: mp 140–141 °C; ^{1}H NMR ($CDCl_3$): δ 7.74 (s, 1H), 7.72 (m, 2H), 7.28 (m, 2H), 5.37 (s, 2H), 2.76 (s, 3H), 2.56 (s, 3H); HRESIMS calcd for $C_{16}H_{13}{}^{81}BrIN_5NaO_2$ *m/z* $[M+Na]^+$ 537.9170, found 537.9181, calcd for $C_{16}H_{13}{}^{79}BrIN_5NaO_2$ *m/z* $[M+Na]^+$ 535.9190 found 535.9196; TLC R_f = 0.50 (40% EtOAc/hexanes); HPLC purity: 99.4%.

4.1.42. 5-(4-Acetyl-5-methyl-1*H*-1,2,3-triazol-1-yl)-4-bromo-2-phenethylpyridazin-3(2*H*)-one (25)

Similar reaction of 2,4-pentanedione (0.40 mL, 3.90 mmol, 1.01 equiv), triethylamine (0.54 mL, 3.87 mmol, 1.00 equiv) and azide **63** (1.236 g, 3.86 mmol, 1.00 equiv) in dry dioxane (60.0 mL; added as a suspension) at 20 °C for 150 min, followed by filtration and evaporation of the filtrate gave a crude product contaminated with the amine derived from **61A**. The mixture was triturated with EtOAc, and the resulting suspension was filtered and the filtrate was evaporated. The residue was purified by column chromatography on silica gel, eluting with 0–40% EtOAc/hexanes, followed by re-precipitation from EtOAc/hexanes, to give **25** (0.187 g, 12%) as a semi-crystalline white solid: mp 150-151 °C; ^{1}H NMR ($CDCl_3$): δ 7.71 (s, 1H), 7.29 (m, 5H), 4.54 (m, 2H), 3.19 (m, 2H), 2.77 (s, 3H), 2.57 (s, 3H); HRESIMS calcd for $C_{17}H_{16}{}^{81}BrN_5NaO_2$ *m/z* $[M+Na]^+$ 426.0360, found 426.0347; calcd for $C_{17}H_{16}{}^{79}BrN_5NaO_2$ *m/z* $[M+Na]^+$ 424.0380, found 424.0367; TLC R_f = 0.52 (40% EtOAc/hexanes); HPLC purity: 99.7%.

4.1.43. 5-(4-Acetyl-5-methyl-1*H*-1,2,3-triazol-1-yl)-4-bromo-2-(3-phenylpropyl)pyridazin-3(2*H*)-one (26)

Similar reaction of 2,4-pentanedione (0.30 mL, 2.92 mmol, 1.00 equiv), triethylamine (0.41 mL, 2.94 mmol, 1.01 equiv) and azide **64** (0.976 g, 2.92 mmol, 1.00 equiv) in dry dioxane (20.0 mL) at 20 °C for 280 min, followed by evaporation of the mixture under reduced pressure and purification of the residue by column chromatography on silica gel, eluting with 0–40% EtOAc/hexanes, gave **26** (0.531 g, 44%) as a pale yellow gummy resin: ^{1}H NMR ($CDCl_3$): δ 7.72 (s, 1H), 7.25 (m, 5H), 4.35 (app t, *J* = 7.3 Hz, 2H), 2.77 (m, 5H), 2.57 (s, 3H), 2.26 (app p, *J* = 22.2, 14.8, 7.5 Hz, 2H); HRESIMS calcd for $C_{18}H_{18}{}^{81}BrN_5NaO_2$ *m/z* $[M+Na]^+$ 440.0516, found 440.0523;

calcd for $C_{18}H_{18}{}^{79}BrN_5NaO_2$ *m/z* $[M+Na]^+$ 438.0536, found 438.0540; TLC R_f = 0.41 (40% EtOAc/hexanes); HPLC purity: 98.4%.

4.1.44. 5-(4-Acetyl-5-methyl-1*H*-1,2,3-triazol-1-yl)-4-bromo-2-(4-((2-(dimethylamino)ethyl)-amino)benzyl)pyridazin-3(2*H*)-one (27)

Using a general literature method,[38] iodide **24** (150 mg, 0.29 mmol, 1.00 equiv), CuI (20 mg, 0.17 mmol, 0.34 equiv), 2-dimethylaminoethylamine (80 μL, 0.74 mmol, 2.55 equiv) and L-proline (20 mg, 0.17 mmol, 0.60 equiv) were combined in dry DMSO (1.0 mL), and the resulting royal blue solution was deoxygenated by three freeze-evacuate-thaw cycles. The reaction mixture was then heated at 95 °C for 5 min, then K_2CO_3 (111 mg, 0.80 mmol, 2.75 equiv) was added, and the resulting mixture deoxygenated by a second series of three freeze-evacuate-thaw cycles, and finally stirred at 95 °C for 16 h. The mixture was cooled, diluted with dry DMSO and filtered through Celite® and the pad washed with a small amount of EtOAc. The combined filtrate was washed with brine (×3), dried (Na_2SO_4), filtered and evaporated under reduced pressure. The crude product from this and a second, 3-fold larger, reaction were combined and purified by column chromatography on silica gel, eluting with 0–20% MeOH:CH_2Cl_2, containing 0.5% v/v aq NH_3 solution (twice), and then by preparative HPLC. The product material thus obtained was unstable as the free base, so was dissolved in saturated aqueous $NaHCO_3$ (pH ~ 8), filtered, the solids washed with EtOAc, and the aqueous filtrate extracted with EtOAc (×4). The combined organic extracts were dried ($MgSO_4$) and evaporated, and the residue was dissolved in a minimum amount of dry MeOH and solution was diluted with ~3 equiv of methanolic HCl followed by EtOAc/hexanes, afforded **27** (diHCl salt) as an amorphous white hygroscopic solid (36 mg, 23%): mp 101–104 °C (powder→glue), 149–153 °C (glue→liquid); ^{1}H NMR ($CDCl_3$): δ 10.00 (v. br s, 2H), 7.55 (s, 1H), 7.51 (d, *J* = 8.3 Hz, 2H), 7.32 (d, *J* = 8.3 Hz, 2H), 5.29 (s, 2H), 3.72 (br s, 2H), 3.30 (br s, 2H), 2.83 (s, 3H), 2.74 (s, 3H), 2.59 (s, 3H), 2.27 (s, 3H) [–NH– not visible]; HRESIMS calcd for $C_{20}H_{25}{}^{81}BrN_7O_2$ *m/z* $[M+H]^+$ 476.1228, found 476.1235, $C_{20}H_{25}{}^{79}BrN_7O_2$ *m/z* $[M+H]^+$ 474.1248, found 474.1251; TLC R_f = 0.29 (10% MeOH:HCl+2 drops aqueous NH_3); HPLC purity: 94.6%.

4.2. Biology experimental

4.2.1. Purification of recombinant PFKFB3

GST-tagged human PFKFB3 was expressed in *Escherichia coli* BL21(DE3) and purified using glutathione sepharose 4 Fast flow beads (GE Healthcare). The resulting pure protein was concentrated to 10 mg mL^{-1} protein at pH 7.4, in a mixture of 50 mm Tris-HCl, 150 mM NaCl, 0.1 mM EDTA, 1 mM DTT and 0.01% TX-100.

4.2.2. PFKFB3 assay protocol

Kinase-Glo® assays (Promega) were performed in assay buffer (40 mM Tris pH 7.5, 20 mM $MgCl_2$, 0.1 mg mL^{-1} BSA) using white 96-well plates. In a typical assay, 10 μL of test compound and 20 μL of PFKFB3 were added to each well and incubated for 30 min at 30 °C. 20 μL of assay buffer containing 25 μM ATP and 1.25 mM F6P were subsequently added to each well. After a 60 min incubation at 30 °C the enzymatic reaction was stopped by addition of 50 μL Kinase-Glo® reagent. Luminescence was recorded using a FLUOstar OPTIMA (BMG Labtech). Data and enzyme kinetics analysis using nonlinear regression was performed using GraphPad Prism (GraphPad Software Inc., San Diego, CA).

4.2.3. Chemical library

Our lead discovery chemical library is a collection of ~87,000 compounds purchased from commercial vendors and stored in neat DMSO at a final compound concentration of 10 mM. The compounds represent a diverse set of molecules, as judged by Tanimoto dissimilarity analysis (Tanimoto dissimilarity *T* value 0.85), and although simple filters based on the Lipinski criteria were not used in the selection process, 89% of the compounds in the library are Lipinski compliant[39] and 81% conform with Oprea's criteria for 'lead likeness'.[40] The screen was carried out at the High Throughput Chemical Screening Facility at the Walter and Eliza Hall Institute in Melbourne, Australia, using the above described Kinase-Glo assay with a fixed compound concentration of 20 μM.

4.2.4. Effect of inhibitors on glycolysis

MDA-MB-231 cells were seeded into Seahorse Bioscience XF24 microplates for 24 h at an initial density of 15,000 cells/well. The medium was then changed to assay medium, and the cells were loaded into the XF24. After 2 baseline measurements, 10 μM of **1** or **7**, or 100 μM of iodoacetate was injected. The response to ECAR was then monitored for 2 h. Then, as a positive control, 100 mM of 2-deoxyglucose was injected and the response to ECAR was monitored for a further 32 min. After the run, cells were lysed in RIPA buffer and protein content was determined by a BCA assay. ECAR was expressed as percentage of baseline measurement.

4.2.5. Molecular docking

The X-ray structure for human PFKFB3 (PDB code 2AXN) was used to predict possible binding modes of 7. All water molecules were removed, hydrogens were added and the side chains of Asn59, Asn69, Asn163, Asn259, Asn321, Gln379, His414 adjusted based on MolProbity[41] using the BIOPOLYMER module of SYBYL. Ligands were prepared by using CONCORD as implemented in SYBYL, and docked into an 18Å cavity centred on the Cα of Gly46 in the nucleotide phosphate binding site using GOLD(v5.1)[41] with the ChemPLP[42] scoring function with set_protein_atom_types turned on. Ligand flexibility options included flip_free_corners, flip_amide_bonds and flip_pyrimidal_n, all other settings were kept at default values.

Acknowledgments

D.G.B., J.U.F. and W.A.D. thank Cancer Society Auckland and the Maurice Wilkins Centre for support.

References and notes

1. Warburg, O. *Science* **1956**, *124*, 269.
2. Hanahan, D.; Weinberg, R. A. *Cell* **2011**, *144*, 646.
3. Griffiths, L. *BMC Proceed.* **2005**, *18*, 321.
4. Potter, V. R. *Fed. Proc.* **1958**, *17*, 691.
5. Vander Heiden, M. G.; Cantley, L. C.; Thompson, C. B. *Science* **2009**, *324*, 1029.
6. Yalcin, A.; Telang, S.; Clem, B.; Chesney, J. *Exp. Mol. Path.* **2009**, *86*, 174.
7. Clem, B.; Telang, S.; Clem, A.; Yalcin, A.; Meier, J.; Simmons, A.; Rasku, M. A.; Arumugam, S.; Dean, W. L.; Eaton, J.; Lane, A.; Trent, J. O.; Chesney, J. *Mol. Cancer Ther.* **2008**, *7*, 110.
8. Wu, C.; Khan, S. A.; Peng, L. J.; Lange, A. J. *Adv. Enzyme Regul.* **2006**, *46*, 72.
9. Sakakibara, R.; Kato, M.; Okamura, N.; Nakagawa, T.; Komada, Y.; Tominaga, N.; Shimojo, M.; Fukasawa, M. *J. Biochem.* **1997**, *122*, 122.
10. Hamilton, J. A.; Callaghan, M. J.; Sutherland, R. L.; Watts, C. K. *Mol. Endocrinol.* **1997**, *11*, 490.
11. Bando, H.; Atsumi, T.; Nishio, T.; Niwa, H.; Mishima, S.; Shimizu, C.; Yoshioka, N.; Bucala, R.; Koike, T. *Clin. Cancer Res.* **2005**, *11*, 5784.
12. Obach, M.; Navarro-Sabate, A.; Caro, J.; Kong, X.; Duran, J.; Gomez, M.; Perales, J. C.; Ventura, F.; Rosa, J. L.; Bartrons, R. *J. Biol. Chem.* **2004**, *279*, 53562.
13. http://atlasgeneticsoncology.org/Genes/PFKFB3ID45932ch10p15.html.
14. Chesney, J.; Mitchell, R.; Benigni, F.; Bacher, M.; Spiegel, L.; Al-Abed, Y.; Han, J. H.; Metz, C.; Bucala, R. *Proc. Natl. Acad. Sci. U.S.A.* **1999**, *96*, 3047.
15. Almeida, A.; Moncada, S.; Bolanos, J. P. *Nat. Cell Biol.* **2004**, *6*, 45.
16. Telang, S.; Yalcin, A.; Clem, A. L.; Bucala, R.; Lane, A. N.; Eaton, J. W.; Chesney, J. *Oncogene* **2006**, *25*, 7225.
17. Clem, B. F.; O'Neal, J.; Tapolsky, G.; Clem, A. L.; Imbert-Fernandez, Y.; Kerr, D. A.; Klarer, A. C.; Redman, R.; Miller, D. M.; Trent, J. O.; Telang, S.; Chesney, J. *Mol. Cancer Ther.* **2013**, *12*, 1461.
18. Chand, P.; Chesney, J. A.; Clem, B. F.; Tapolsky, G. H.; Telang, S.; Trent, J. O. WO 2011/103557 A1, published 25th August 2011.

19. Kim, S.-G.; Manes, N. P.; El-Maghrabi, M. R.; Lee, Y.-H. *J. Biol. Chem.* **2006**, *281*, 2939.
20. Seo, M.; Kim, J.-D.; Neau, D.; Sehgal, I.; Lee, Y.-H. *PLoS ONE* **2011**, *6*, e24179.
21. Crochet, R. B.; Cavalier, M. C.; Seo, M.; Kim, J.-D.; Yim, Y.-S.; Park, S.-J.; Lee, Y.-H. *Anal. Biochem.* **2011**, *418*, 143.
22. Angbrant, J.; Homan, E.; Lundbaeck, T.; Martinsson, J.; Sari, M.; Joensson, M.; Faernegaardh, K.; Hallberg, K. WO 2011/161201 A1, published 29th December 2011.
23. Solov'eva, V. V.; Gudriniece, E. Latvijas PSR Zinatnu Akademijas Vestis, Kimijas Serija 1972, 5, 572–575. (*Chem. Abstr.* **1973**; 16120).
24. Humphries, P. S.; Oliver, R. M. *Tetrahedron Lett.* **2009**, *50*, 2682.
25. Krajsovszky, G.; Károlyházy, L.; Reidl, Zs.; Csámpai, A.; Dunkel, P.; Lernyei, Á.; Dajka-Halász, B.; Hajós, Gy.; Mátyus, P. *J. Mol. Struct.* **2005**, *713*, 235.
26. Ryabtsova, O.; Verhelst, T.; Baeten, M.; Vande Velde, C. M. L.; Maes, B. U. W. *J. Org. Chem.* **2009**, *74*, 9440.
27. Chang, H. K.; Oh, Y. S.; Jang, Y. J. WO 2008/016239, published 7th February 2008.
28. Devraj, R.; Hepperle, M.; Jerome, K.; Selness, S.; Walker, J. K. WO 2005/007632 A1, published 27th January 2005.
29. Qian, W.; Winternheimer, D.; Allen, J. *Org. Lett.* **2011**, *13*, 1682.
30. Wilcken, R.; Zimmermann, M. O.; Lange, A.; Joerger, A. C.; Boeckler, F. M. *J. Med. Chem.* **2013**, *56*, 1363.
31. Hansch, C.; Leo, A. *Substituent Constants for Correlation Analysis in Chemistry and Biology*; Wiley Interscience: NY, ISBN 0-471-05062-8, 1979.
32. Wu, M.; Neilson, A.; Swift, A. L.; Moran, R.; Tamagnine, J.; Parslow, D.; Armistead, S.; Lemire, K.; Orrell, J.; Teich, J.; Chomicz, S.; Ferrick, D. A. *Am. J. Physiol. Cell Physiol* **2007**, *292*, C125.
33. Meier, K.; Ringier, B. H.; Druey, J. *Helv. Chim. Acta* **1954**, *37*, 523.
34. Banner, D.; Ceccarelli, S. M.; Grether, U.; Haap, W.; Hilpert, H.; Kuehne, H.; Mauser, H.; Plancher, J.-M., Sanchez, R. A. WO 2010/142650 A1, published 16th December 2010.
35. Wuitschik, G.; Rogers-Evans, M.; Buckl, A.; Bernasconi, M.; Märki, M.; Godel, T.; Fischer, H.; Wagner, B.; Parrilla, I.; Schuler, F.; Schneider, J.; Alker, A.; Schweizer, W. B.; Müller, K.; Carreira, E. M. *Angew. Chem., Int. Ed.* **2008**, *47*, 4512.
36. Kamalraj, V. R.; Senthil, S.; Kannan, P. *J. Mol. Struct.* **2008**, *892*, 210.
37. Ting, P. C.; Aslanian, R. G.; Cao, J.; Kim, D. W.-S.; Kuang, R.; Zhou, G.; Herr, R. J.; Zych, A. J.; Yang, J.; Wu, H.; Zorn, N. WO 2008/115381 A1, published 25th September 2008.
38. Lipinski, C. A.; Lombardo, F.; Dominy, B. W.; Feeney, P. J. *Adv. Drug Deliv. Rev.* **2001**, *46*, 3.
39. Oprea, T. I.; Davis, A. M.; Teague, S. J.; Leeson, P. D. *J. Chem. Infect. Comput. Sci.* **2010**, *41*, 1308.
40. Chen, V. B.; Arendall, W. B.; Headd, J. J.; Keedy, D. A.; Immormino, R. M.; Kapral, G. J.; Murray, L. M.; Richardson, J. S.; Richardson, D. C. *Acta Cryst.* **2010**, *D66*, 12.
41. Jones, G.; Willett, P.; Glen, R. C.; Leach, A. R.; Taylor, R. J. *Mol. Biol.* **1997**, *267*, 727.
42. Liebeschuetz, J. W.; Cole, J. C.; Korb, O. *J. Comput. Aided Mol. Des.* **2012**, *26*, 737.